Appl. Phys. A 90, 329–331 (2008)
DOI: 10.1007/s00339-007-4277-1

Applied Physics A
Materials Science & Processing

CHENG-FU YANG[1]
KAI-HUANG CHEN[2]
YING-CHUNG CHEN[3,✉]
TING-CHANG CHANG[4]

Physical and electrical characteristics of $Ba(Zr_{0.1}Ti_{0.9})O_3$ thin films under oxygen plasma treatment for applications in nonvolatile memory devices

[1] Department of Chemical and Materials Engineering, National University of Kaohsiung, Kaohsiung 804, Taiwan, R.O.C.
[2] Department of Electronics Engineering and Computer Science, Tung-Fang Institute of Technology, Kaohsiung 804, Taiwan, R.O.C.
[3] Department of Electrical Engineering, National Sun Yat-Sen University, Kaohsiung 804, Taiwan, R.O.C.
[4] Department of Physics, National Sun Yat-sen University, Kaohsiung 804, Taiwan, R.O.C.

Received: 24 April 2007/Accepted: 4 August 2007
Published online: 25 September 2007 • **© Springer-Verlag 2007**

ABSTRACT In this study, the effects of oxygen gas plasma treatment on the surface of $Ba(Zr_{0.1}Ti_{0.9})O_3$ (BZT) films are investigated. The influence of oxygen plasma treatment on the crystal structure is developed by X-ray diffraction patterns and on the electrical characteristics are measured by the Al/BZT/Pt capacitor (metal–dielectric–metal) structure. Experimental results show that the capacitance increases and the leakage current density decreases as the oxygen plasma is treated on the BZT films. These results clearly indicate that the electrical characteristics of BZT films have effectively improved by means of the oxygen plasma surface treatment process.

PACS 77.84.-s; 81.15.Cd; 73.40.Qv; 77.22.Ej; 51.50.+v

1 Introduction

Recently, several memory devices such as dynamic random access memory, flash memory, SONOS, FRAM, MRAM, etc., have been developed. Among volatile and nonvolatile memories, the nondestructive readout feature of high-density nonvolatile memories is expected to play an important role in the future [1–3]. The excellent quality insulator of various oxide materials results from defects and oxygen vacancies of the grain boundary. Their electrical and physical characteristics are also affected with regard to their applications in integrated circuits. Thus, the defects and oxygen vacancies existing in conventional oxide films are usually filled and compensated by oxygen gas using different thin film deposition methods in the semiconductor manufacturing process. The crystal structure and grain growth of oxide films can be improved with an increase of deposition temperature. However, the oxygen atoms in the crystal structure of the grain boundary would be destabilised and lost at higher deposition temperatures [4–7].

Several ferroelectric thin films with higher remnant polarizations and lower coercive fields, such as $Pb(Zr, Ti)O_3$ (PZT), $SrBi_2Ta_2O_9$ (SBT), $SrTiO_3$ (ST), and $(Ba, Sr)TiO_3$ (BST), have been widely studied and discussed for applications to higher storage capacity FRAM devices [8–11]. Ferroelectric materials such as $(Ba, Sr)TiO_3$ (BST) and $Ba(Ti, Zr)O_3$ (BZT) films are expected to be an improvement over common PZT or SBT memory materials because of lower pollution problems, lower deposition temperatures, and lower leakage current densities as compared to the those of conventional PZT perovskite films. In this study, we will report and investigate the correlation between the variations in the physical and electrical characteristics of as-deposited BZT films during oxygen plasma treatment.

2 Experimental

In this study, the BZT films were deposited on a $Pt/Ti/SiO_2/Si$ substrate by means of radio frequency (rf) magnetron sputtering using a 2-inch $Ba(Zr_{0.1}Ti_{0.9})O_3$ ceramic target. The target was placed 8 cm away from the substrate. The BZT films deposited in the process for 1 h under the optimal sputtering parameters, namely, an rf power of 160 W, a substrate temperature of 580 °C, a chamber pressure of 10 mTorr and an oxygen concentration of 25%. To complete the metal–ferroelectric–metal (MFM or MFMIS) structure as shown in Fig. 1, an array of circular top contacts with a diameter of 0.1 cm was formed by depositing an Al film, which had a 500 nm thickness and resulted from thermal evaporation. The deposited BZT films were inductively coupled plasma using oxygen as the source gas for different durations. The substrate temperature and total gas pressure in the inductively coupled plasma were maintained at 300 °C and 25 mTorr, respectively. The dielectric constants

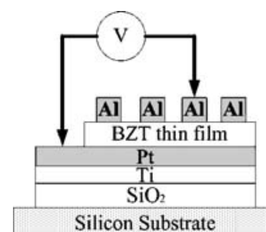

FIGURE 1 The configuration of a MFM structure

✉ Fax: +886-7-5254015, E-mail: ycc@ee.nsysu.edu.tw

and leakage currents of deposited BZT films were measured by using an impendence analyzer (HP 4194A) and a semiconductor parameter analyzer (HP 4156). In addition, the polarization–electrical field (P–E) curves of BZT films were measured using Sawyer–Tower circuits at 100 Hz–1 MHz. X-ray diffraction (SIEMENS D5000) using Cu K_α radiation and Ni filter was used to determine the crystal phase of deposited BZT films. Moreover, the thickness and the surface morphology of films were verified by field effect scanning electron microscopy (FESEM).

3 Results and discussion

Figure 2 shows the (001), (011), (111), (002), and (112) peaks observed from the X-ray diffraction patterns of the deposited BTZ thin films. As the XRD patterns shown in Fig. 2 are compared, the crystal intensities of the oxygen-plasma-treated BZT films are greater than those of the non-plasma-treated ones. We have demonstrated that the oxygen vacancy in of the perovskite structure BZT films would be filled during the oxygen plasma treatment process. From the FESEM observations, the thickness of as-deposited BZT films are about 450–490 nm (not shown here). Based on the surface image shown in Fig. 3 and the SEM cross-section, the grain size and the deposition rate of the BZT films are calculated to be approximately 30–60 nm and 7.5–8.2 nm/min, respectively. Figure 3 also shows that the deposited BZT films reveal a denser structure and almost no pores are observed. The thickness and grain size of the BZT films is not changed by the oxygen plasma treatment used.

Figure 4 compares the change of the capacitance versus the applied voltage (C–V) for the non-plasma-treated and oxygen-plasma-treated BZT films. Based on Fig. 4, the capacitances increase from 1.85 to 2.45 nF as the oxygen-plasma-treated time increases from 0 min to 6 min. As suggested by Fig. 2, the improvement in the dielectric constants of BZT films can be attributed to the compensation of the oxygen vacancy and the improvement in the crystallization of the ABO_3 phase in the BZT films.

Figure 5 shows the leakage current density versus applied voltage (J–V) curves of the BZT films. For non-plasma-treated BZT films, the leakage current density increases slightly as the applied field increases from 0 MV/cm to 0.12 MV/cm and increases critically as the applied field in-

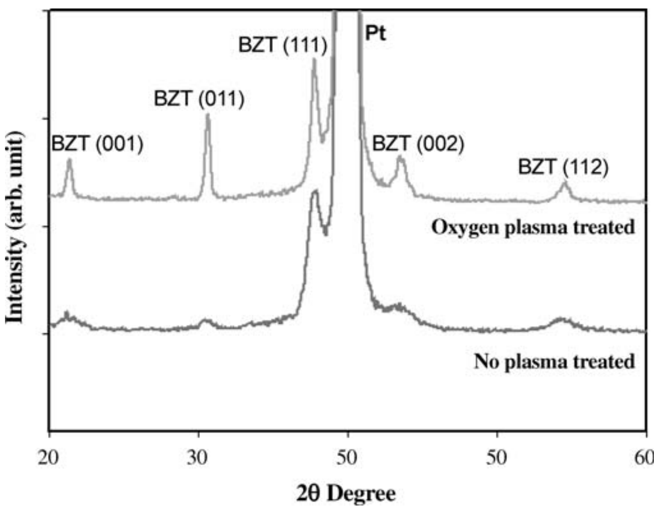

FIGURE 2 Variations in the peak intensities of the oxygen-plasma-treated BZT films

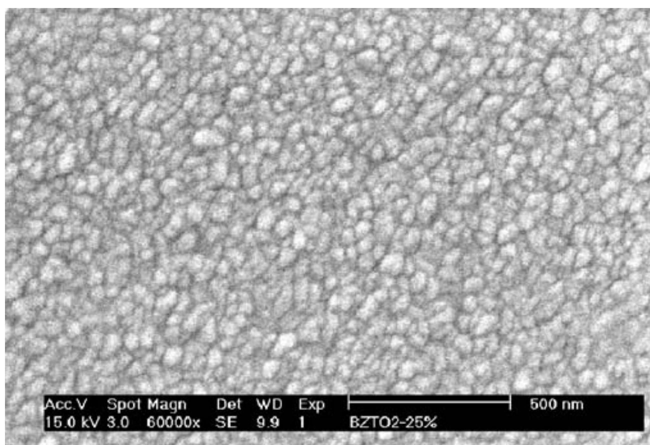

FIGURE 3 The SEM surface images of BZT films

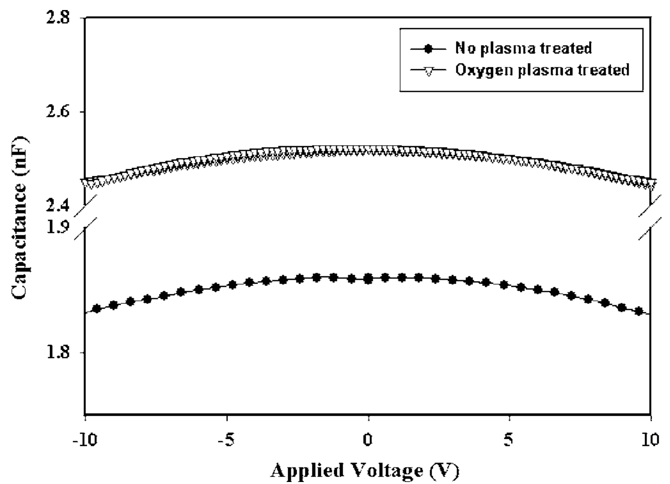

FIGURE 4 The capacitance versus applied voltage curves of the non-plasma-treated and plasma-treated BZT films

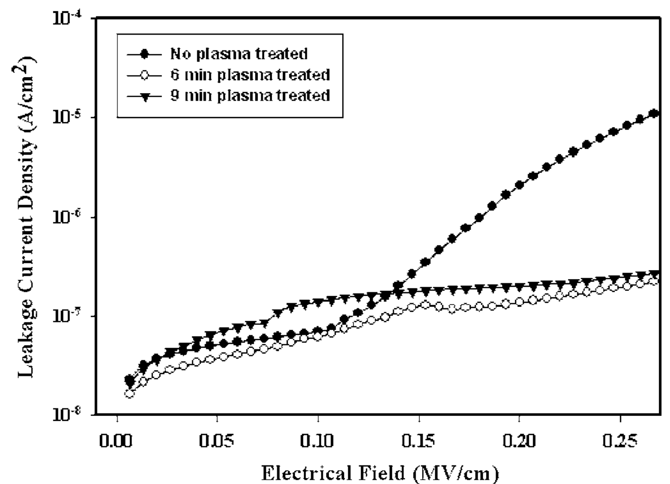

FIGURE 5 The leakage current density versus electrical field of non-plasma-treated and plasma-treated BZT films

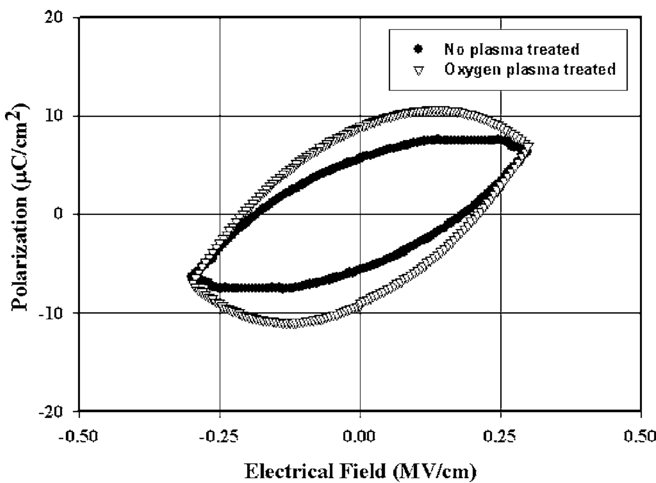

FIGURE 6 The polarization versus electrical field of non-plasma-treated and plasma-treated BZT films

creases from 0.12 MV/cm to 0.27 MV/cm. As shown in Fig. 5, since the applied field is higher than 0.13 MV/cm, the leakage current densities of the oxygen-plasma-treated BZT films have a lower value than that of the non-plasma-treated ones. At an electric field of 0.25 MV/cm, the oxygen-plasma-treated films exhibit a leakage current density two orders of magnitude lower than those of the non-plasma-treated ones. As mentioned above, the oxygen plasma treatment decreases the oxygen vacancies and the leakage current density and then increases the capacitances of the BZT films. The current-field curves shown in Fig. 5 are fit to Schottky emission and Poole–Frankel transport models to determine the reason for the observed decrease in leakage current of the oxygen plasma treated films [12, 13]. Smyth et al. reported that as the dielectric films had a longer oxygen-plasma-treated process, the excess O_2 will escape during plasma processing according to (1)

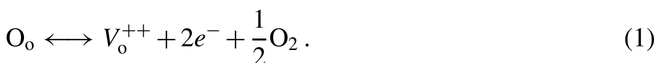

$$O_o \longleftrightarrow V_o^{++} + 2e^- + \frac{1}{2}O_2 \,. \qquad (1)$$

Here O_o, V_o^{++}, and e^- are, the oxygen ion at its normal site, an oxygen vacancy, and an electron, respectively [14]. The oxygen vacancies will increase after 9 min oxygen plasma treatment and that will cause the slight increase in the leakage current density.

Figure 6 shows *P–E* curves of the BZT films observed at a frequency of 100 kHz under an applied electrical field of 0–0.28 MV/cm. After oxygen plasma treatment, the coercive field has no apparent change; however, the remnant polarization increases from 6 to 9 μC/cm^2. As shown in Fig. 6, the saturation polarization decreases slightly when an electrical field of 0.280 MV/cm is applied. This effect can be caused by the higher leakage current density under larger electrical fields.

4 Conclusion

In this report, the crystal intensities of ABO_3 phase in BZT films have been improved after the oxygen plasma treatment. In addition, the oxygen-plasma-treated BZT films have a higher capacitance (dielectric constant) of 2.45 nF and a lower leakage current density of 10^{-7} MV/cm, respectively. The improvement in the remnant polarization of the BZT films by oxygen plasma treatment is also observed. Therefore, the superior electrical characteristics of BZT films can be obtained by the oxygen-plasma-treated process. Additionally, the oxygen-plasma-treated process is expected to play an important role for their future applications in nonvolatile memory devices.

ACKNOWLEDGEMENTS This study is partly supported by the National Science Council under contract Nos. NSC 95-2221-E-110-029 and NSC 95-2221-E-390-009.

REFERENCES

1 S.Y. Wu, IEEE Trans. Electron. Dev. **21**, 499 (1974)
2 S.Y. Wu, Ferroelectrics **11**, 379 (1976)
3 H. Buhay, S. Sinharoy, W.H. Kasner, M.H. Francombe, D.R. Lampe, E. Stepke, Appl. Phys. Lett. **58**, 1470 (1991)
4 S.R. Shannigrahi, H.M. Jang, Appl. Phys. Lett. **79**, 1051 (2001)
5 S. Kamiyama, H. Suzuki, H. Watanabe, A. Sakai, M. Oshida, T. Tatsumi, T. Tanigawa, N. Kasai, A. Ishitani, IEEE Int. Electron Devices Meet. (1993), p. 49
6 S.C. Sun, T.F. Chen, IEEE Electron. Dev. Lett. **17**, 355 (1996)
7 Y. Fukuda, K. Numata, K. Aoki, A. Nishimura, G. Fujihashi, Japan. J. Appl. Phys. **37**, 453 (1998)
8 S.K. Hong, C.W. Suh, C.G. Lee, S.W. Lee, E.Y. Hang, N.S. Kang, Appl. Phys. Lett. **77**, 76 (2000)
9 S.B. Xiong, S. Sakai, Appl. Phys. Lett. **75**, 1613 (1999)
10 J.S. Kim, S.G. Yoon, J. Vac. Soc. Technol. B **18**, 216 (2000)
11 T.B. Wu, C.M. Wu, M.L. Chen, Appl. Phys. Lett. **69**, 2659 (1996)
12 S. Fleischer. P.T. Lai, Y.C. Cheng, J. Appl. Phys. **73**, 8353 (1994)
13 P. Hesto, in *Instabilities in Silicon Devices: Silicon Passivation and Related Instabilities*, ed. by G. Barbottin, A. Vapaille (Elsevier, North Holland, 1986), p. 263
14 D.M. Smyth, M.P. Harmer, P.J. Peng, J. Am. Ceram. Soc. **72**, 2276 (1989)